0026-895X/07/7206-1535–1544$20.00
MOLECULAR PHARMACOLOGY
Copyright © 2007 The American Society for Pharmacology and Experimental Therapeutics
Mol Pharmacol 72:1535–1544, 2007

Vol. 72, No. 6
40071/3278985
Printed in U.S.A.

The N-Terminal Domains of both NR1 and NR2 Subunits Determine Allosteric Zn^{2+} Inhibition and Glycine Affinity of *N*-Methyl-D-aspartate Receptors

Christian Madry, Ivana Mesic, Heinrich Betz, and Bodo Laube

Abteilung Neurochemie, Max-Planck-Institut für Hirnforschung, Frankfurt am Main, Germany (C.M., I.M., H.B., B.L.); and AG Molekulare und Zelluläre Neurophysiologie, Technische Universität Darmstadt, Darmstadt, Germany (I.M., B.L.)

Received July 16, 2007; accepted September 17, 2007

ABSTRACT

The *N*-methyl-D-aspartate (NMDA) subtype of ionotropic glutamate receptors (iGluRs) is a tetrameric protein composed of homologous NR1 and NR2 subunits, which require the binding of glycine and glutamate, respectively, for efficient channel gating. The extracellular N-terminal domains (NTDs) of iGluR subunits show sequence homology to the bacterial periplasmic leucine/isoleucine/valine binding protein (LIVBP) and have been implicated in iGluR assembly, trafficking, and function. Here, we investigated how deletion of the NR1- and NR2-NTDs affects the expression and function of NMDA receptors. Both proteolytic cleavage of the NR1-NTD from assembled NR1/NR2 receptors and coexpression of the NTD-deleted NR1 subunit with wild-type or NTD-deleted NR2 subunits resulted in agonist-gated channels that closely resembled wild-type receptors. This indicates that the NTDs of both NMDA receptor subunits are not essential for receptor assembly and function. However, deletion of either the NR1 or the NR2 NTD eliminated high-affinity, allosteric inhibition of agonist-induced currents by Zn^{2+} and ifenprodil, consistent with the idea that interdomain interactions between these domains are important for allosteric receptor modulation. Furthermore, by replacing the NR2A-NTD with the NR2B NTD, and vice versa, the different glycine affinities of NR1/NR2A and NR1/NR2B receptors were found to be determined by their respective NR2-NTDs. Together, these data show that the NTDs of both the NR1 and NR2 subunits determine allosteric inhibition and glycine potency but are not required for NMDA receptor assembly.

Excitatory neurotransmission in the mammalian brain is mainly mediated by ionotropic glutamate receptors (iGluRs). Based on pharmacological studies, iGluRs have been grouped into three distinct subfamilies: AMPA receptors (GluR1–4), kainate receptors (GluR5–7, KA1, 2), and NMDA receptors (NR1, NR2A-D, NR3A, B) (overview in Dingledine et al., 1999; Cull-Candy et al., 2001). All iGluR subunits share a common modular design characterized by 1) an extracellular N-terminal domain (NTD) of approximately 400 amino acids that shows sequence homology to the bacterial periplasmic leucine/isoleucine/valine binding protein (LIVBP) and has been implicated in iGluR subunit oligomerization, trafficking, and function; 2) a S1S2 ligand binding domain (LBD) composed of an extracellular region preceding the first transmembrane domain and a second extracellular region connecting the transmembrane segments 2 and 3; 3) a membrane re-entrant loop domain located between transmembrane segments 1 and 2, which lines the ion channel; and 4) an intracellular carboxyterminal tail region that interacts with postsynaptic scaffolding and signal transduction proteins (reviewed in Madden, 2002).

Among iGluRs, NMDA receptors stand out with respect to both their molecular diversity and their particular pharmacological and functional properties (Dingledine et al., 1999). Within the heterotetrameric receptor proteins, various splice variants of the glycine-binding NR1 subunit (Kuryatov et al., 1994) coassemble with glutamate-binding NR2 (Laube et al., 1997) and/or glycine-binding NR3 subunits (Yao and Mayer, 2006). Activation of NMDA receptors is a complex process

This study was supported by the Max-Planck-Gesellschaft (H.B.), Gemeinnützige Hertie-Stiftung (B.L.), Dr. Robert Pfleger Stiftung (B.L.), Deutsche Forschungsgemeinschaft (grant LA 1086/4-1, B.L.), and Fonds der Chemischen Industrie (H.B.). C.M. received a predoctoral fellowship from the Graduiertenkolleg Neuronale Plastizität, University of Frankfurt.

Article, publication date, and citation information can be found at http://molpharm.aspetjournals.org.

doi:10.1124/mol.107.040071.

ABBREVIATIONS: iGluR, ionotropic glutamate receptor; AMPA, α-amino-3-hydroxy-5-methyl-4-isoxazolepropionic acid ; NMDA, *N*-methyl-D-aspartic acid; NTD, N-terminal domain; LIVBP, leucine/isoleucine/valine binding protein; LBD, ligand binding domain; HEK, human embryonic kidney; ifenprodil, 4-[2-[4-(cyclohexylmethyl)-1-piperidinyl]-1-hydroxypropyl]phenol; MK801, (+)-5-methyl-10,11-dihydro-5*H*-dibenzo[*a*,*d*]cyclohepten-5,10-imine maleate); MDL-29951, 3-(2-carboxyethyl)-4,6-dichloro-1*H*-indole-2-carboxylic acid; PAGE, polyacrylamide gel electrophoresis; EGFP, enhanced green fluorescent protein; TCS, thrombin cleavage site; wt, wild-type; t-PA, tissue-type plasminogen activator.

that requires ambient glycine and release of glutamate from presynaptic terminals in coincidence with postsynaptic membrane depolarization, which relieves the receptor channel from a voltage-dependent block by Mg^{2+} ions. NMDA receptor function is regulated by allosteric inhibitors, such as Zn^{2+} and the phenylethanolamine ifenprodil, which bind to the NTDs of NR2A and NR2B subunits (Herin and Aizenman, 2004) and enhance receptor desensitization (Krupp et al., 1998; Zheng et al., 2001). The molecular basis of allosteric NMDA receptor inhibition is poorly understood but has been attributed to interactions between the NTD and the LBD of the NR2 subunits (Paoletti et al., 2000). Deletion of the NR2A and NR2B NTDs generates NMDA receptors that display a reduced inhibition by both Zn^{2+} and ifenprodil (Paoletti et al., 2000). The role of the NR1-NTD has not been investigated further, because N-terminal truncations within the NR1 subunits have been reported to impair receptor function upon coexpression with NR2 subunits (Meddows et al., 2001).

Here, we analyzed the role of the NTD of the NR1 subunit in NMDA receptor assembly and allosteric inhibition by both enzymatically cleaving this domain from properly assembled receptors and coexpressing a truncated NR1 subunit with wild-type or NTD-deleted NR2A and NR2B subunits. We find that, like the NR2-NTDs, the NR1-NTD is not required for receptor function and assembly but notably contributes to allosteric Zn^{2+} and ifenprodil inhibition. In addition, high-affinity glycine binding requires the NTDs of both NR1 and NR2B subunits. Our data suggest that direct interactions between the NR1 and NR2 NTDs determine the potency of allosteric inhibitors and the coagonist glycine.

Materials and Methods

MK801, D-(−)-2-amino-5-phosphonopentanoic acid, and MDL-29951 were purchased from Tocris (Biotrend, Cologne, Germany). All other chemicals used were obtained from Sigma (Taufkirchen, Germany).

DNA Constructs, Oocyte Expression, and Electrophysiology. cDNAs of the NR1a, NR2A, and NR2B subunits were subcloned into the pNKS2 vector. Mutations were introduced by site-directed mutagenesis (QuikChange XL site-directed mutagenesis kit; Stratagene, Amsterdam, The Netherlands) and confirmed by DNA sequencing. The $NR1^{\Delta NTD}$ construct was generated by excising the nucleotide sequence encoding amino acids 5 to 358 of the mature protein with the use of PvuI. To enzymatically remove the NTD of NR1, a thrombin recognition sequence (LVPRGS) (Madry et al., 2007) was inserted at position 358 of the NR1 subunit that had been fused to enhanced green fluorescent protein ($EGFP\text{-}NR1^{TCS}$) by subcloning into the pEGFP-C1 vector (Clontech, Mountain View, CA). The $NR2A^{\Delta NTD}$, $NR2B^{\Delta NTD}$, $NR2A^{NTD2B}$, and $NR2B^{NTD2A}$ constructs (Paoletti et al., 2000; Rachline et al., 2005) were kindly provided by Dr. P. Paoletti (Ecole Normale Supérieure, Paris, France). The NR2A*-His construct was generated by replacing the C-terminal region from amino acid 930 with a 6× His tag (Madry et al., 2007). In vitro synthesis of cRNA (mCAP mRNA Capping Kit; Ambion, Austin, TX) was performed as described previously (Madry et al., 2007). For heterologous expression of NMDA receptors, 25 ng of cRNA was injected at a NR1:NR2 ratio of 1:2 into *Xenopus laevis* oocytes. Oocytes were isolated and maintained as described previously (Laube et al., 1997). Two-electrode voltage-clamp recording of whole-cell currents was performed according to Laube et al. (1995). To monitor the voltage dependence of NR1/NR2B NTD-deleted receptor combinations, 2-s −80/+40 mV voltage ramps were used. Leakage currents were recorded before agonist/Zn^{2+} application and subtracted from the agonist/Zn^{2+} -induced currents. To measure desensitization of receptor responses, we recorded currents upon application of saturating concentrations of glycine and glutamate (100 μM, each) until a steady-state plateau was reached. Based on steady-state (I_{ss}) and peak (I_p) current amplitudes recorded in the same solution, we calculated the extend of desensitization as the percentage (%) of current decay in the continuous presence of the agonists. For thrombin treatment, oocytes were incubated with 30 U/ml protease for 60 min at room temperature. Same oocytes were measured before and after thrombin exposure.

Transfection of HEK293 Cells and Thrombin Treatment. Culture conditions for human embryonic kidney (HEK) 293 cells (American Type Culture Collection, Manassas, VA) have been described previously (Laube et al., 1995). Transfection with Lipofectamine 2000 was performed according to the manufacturer's protocol (Invitrogen, Carlsbad, CA). HEK293 cells were cotransfected with either EGFP-NR1 (wt) or $EGFP\text{-}NR1^{TCS}$ plasmid together with the NR2A construct, using 20 μg of total DNA at a NR1/NR2 ratio of 1:3. Transfected cells were cultured in the presence of the NMDA inhibitors MK801, D-(−)-2-amino-5-phosphonopentanoic acid, and MDL-29951 (all 100 μM) for 48 h. Then new medium without Ca^{2+} and bovine serum albumin was added, and the cells were incubated with 30 U/ml thrombin for 30 min at 37°C followed by harvesting and homogenization in a Polytron homogenizer (Kinematica, Basel, Switzerland). After centrifugation at 1000*g*, the supernatant was centrifuged at 10,000*g* for 20 min at 4°C to obtain the membrane pellet, which then was suspended in SDS sample buffer.

Metabolic Labeling, Purification, and SDS-PAGE of NMDA Receptor Complexes. Injected oocytes were metabolically labeled by overnight incubation with [^{35}S]methionine as described previously (Madry et al., 2007). After an additional 24-h chase interval, labeled receptor complexes were purified by nickel-nitrilotriacetic acid chromatography from 0.5% (w/v) dodecylmaltoside extracts of the labeled oocytes as detailed previously (Sadtler et al., 2003). For SDS-PAGE, protein samples were solubilized in SDS sample buffer containing 20 mM dithiothreitol and electrophoresed in parallel with molecular mass markers (Precision Plus Protein All Blue Standard; Bio-Rad Laboratories, Munich, Germany) on 10% Tricine/SDS-polyacrylamide gels. Radioactive gels were dried and exposed to BioMax MR films (Kodak, Stuttgart, Germany) at 80°C or to a phosphor-imaging plate for quantification purposes. Phosphor plates were scanned on a Typhoon Trio fluorescence scanner and analyzed with Image Quant TL software (GE Healthcare, Chalfont St. Giles, Buckinghamshire, UK).

Antibodies. Anti-NR1 (generated against amino acids 660–811 of the rat NR1 subunit) and anti-EGFP primary antibodies were purchased from BD Biosciences (Heidelberg, Germany) and used at dilutions of 1:500 (NR1) and 1:1000 (EGFP), respectively. Goat anti-mouse horseradish peroxidase-linked secondary antibody (Dianova, Hamburg, Germany) was employed at a final dilution of 1:10,000, and immunoreactive bands were detected with the ECL Western blotting system (GE Healthcare, Munich, Germany).

Statistical Analyses. Values given represent means ± S.E. Statistical significance was determined at the $p < 0.01$ (*) and $p < 0.001$ (**) levels using a Student's two-tailed, unpaired *t* test.

Results

To investigate the role of the NTD of the glycine-binding NR1 subunit in NMDA receptor assembly and function, we designed two different NR1 cDNA constructs. First, by inserting a thrombin cleavage site (TCS) sequence at amino acid position 358 of the NR1 subunit ($EGFP\text{-}NR1^{TCS}$; Fig. 1A), we generated a NR1 subunit, which should allow proteolytic cleavage of the NR1-NTD from surface-located receptors upon thrombin treatment. Visualization and immunological detection of the respective NR1-NTD fragment was achieved by an N-terminal EGFP tag (see Fig. 1A, and *Materials and Methods*). Second, a truncated NR1 subunit

(NR1$^{\Delta NTD}$; Fig. 1A) was generated by deleting the nucleotide sequence encoding residues 5 to 358.

Biochemical and Functional Characterization of NMDA Receptors Containing the Thrombin-Cleavable EGFP-NR1^{TCS} Subunit. To examine whether the NR1^{TCS} construct is cleaved by thrombin, we coexpressed both the EGFP-NR1 and the EGFP-NR1^{TCS} subunits with the NR2A subunit in HEK 293 cells. Western blot analysis of membrane fractions prepared from the transfected cells revealed a single band of apparent molecular mass of approximately 130 kDa with both the wild-type (wt) EGFP-NR1 and the EGFP-NR1^{TCS} DNAs upon staining with an anti-EGFP antibody (Fig. 1B, lanes 1 and 2). Upon thrombin treatment of the intact cells, membranes prepared from wt EGFP-NR1 and NR2A transfected cells again contained a 130-kDa NR1 protein band that was recognized by both anti-NR1 and anti-EGFP antibodies (Fig. 1B, lanes 3 and 4). In contrast, treatment of EGFP-NR1^{TCS} and NR2A subunit-expressing cells with thrombin generated, in addition to the 130-kDa band, two prominent fragments of approximately 60 and 70 kDa that were stained by anti-NR1 and anti-EGFP, respectively (Fig. 1B, lanes 5 and 6). These fragment sizes are consistent with the calculated masses of the membrane-bound "core" NR1 subunit and the truncated EGFP-tagged NTD of the EGFP-NR1^{TCS} subunit (Fig. 1A). This indicates an efficient cleavage of surface-located EGFP-NR1^{TCS}/NR2A receptors, whereas the noncleaved NR1^{TCS} 130-kDa protein most likely corresponds to thrombin-inaccessible intracellularly located subunits. Furthermore, copurification of the truncated EGFP-tagged NTD in the membrane fraction shows that cleavage of the NR1-NTD by thrombin does not necessarily result in a separation of this domain from the "core" receptor, implying strong noncovalent interactions with the remaining protein.

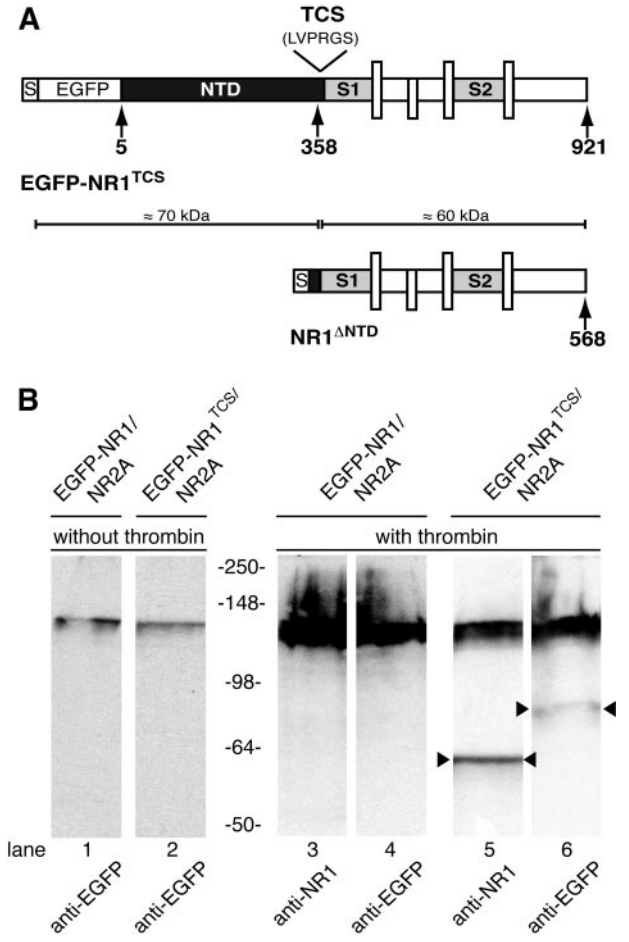

Fig. 1. Biochemical characterization of a thrombin-cleavable NR1^{TCS} subunit. A, schematic representations of 1) an NR1 construct harboring a thrombin clevage site (LVPRGS) at amino acid position 358 and an N-terminal EGFP-tag (EGFP-NR1^{TCS}, top) and 2) an NTD-deleted NR1 subunit lacking amino acids 5–358 (NR1$^{\Delta NTD}$, bottom). S, signal peptide (18 amino acids); S1S2, glycine binding domains. Hydrophobic intramembrane regions are indicated as vertical boxes. Amino acid numbering starts with the first amino acid of the mature protein. B, left, Western blot analysis of wt EGFP-NR1 and EGFP-NR1^{TCS} proteins generated upon coexpression with the NR2A subunit in HEK 293 cells. A single band of approximately 130-kDa molecular mass is detected using the anti-EGFP antibody (lanes 1 and 2). Right, thrombin treatment of EGFP-NR1^{TCS}-expressing HEK 293 cells for 30 min resulted in the appearance of 70-kDa N-terminal and 60-kDa C-terminal fragments that reacted with the anti-EGFP and anti-NR1 antibodies, respectively (lanes 5 and 6). In contrast, the wt EGFP-NR1 subunit was not cleaved by thrombin under the same conditions (lanes 3 and 4).

The consequences of thrombin-mediated cleavage of the NR1-NTD on apparent agonist affinities and maximal inducible currents (I_{max}) were analyzed by two-electrode voltage clamping after coexpression of EGFP-NR1^{TCS} with the NR2B subunit in *Xenopus laevis* oocytes. The resulting glycine and glutamate dose-response curves were indistinguishable to those of the wt NR1/NR2B receptor in the absence and presence of thrombin. In contrast, after thrombin treatment, the EC_{50} value of the EGFP-NR1^{TCS}/NR2B receptor showed a significant decrease in apparent glycine affinity (0.30 ± 0.04 versus 0.80 ± 0.14 μM; $p < 0.01$, $n = 4$), whereas the glutamate EC_{50} value (1.2 ± 0.4 versus 1.3 ± 0.3 μM) and the maximal inducible currents were not significantly changed (Fig. 2A, left). Because a similar result was also obtained for EGFP-NR1^{TCS}/NR2A receptors (Fig. 2B, left), we conclude that thrombin-mediated cleavage of the NR1 NTD does not impair receptor function.

Cleavage of the NR1-NTD Eliminated High-Affinity Zn^{2+} Inhibition of NR1/NR2 Receptors. Because the NTDs of the NR2 subunits have been found to mediate the allosteric inhibition of NMDA receptors (overview in Herin and Aizenman, 2004), we also examined the effect of thrombin-mediated NR1-NTD deletion on Zn^{2+} inhibition of both EGFP-NR1^{TCS}/NR2B and EGFP-NR1^{TCS}/NR2A receptor currents. NR2B-containing NMDA receptors are inhibited by micromolar concentrations of Zn^{2+} (Rachline et al., 2005). Upon thrombin treatment of oocytes expressing the EGFP-NR1^{TCS}/NR2B combination, the IC_{50} value of Zn^{2+} increased 19-fold, from 13 ± 3 μM before to 256 ± 34 μM after incubation with the protease ($p < 0.01$, $n = 3$; Fig. 2A, right). This suggested that the NTD of the NR1 subunit is not essential for receptor function but contributes to allosteric Zn^{2+} inhibition.

To examine whether the NR1-NTD is also required for the biphasic mode of Zn^{2+} inhibition seen with NR1/NR2A receptors (Williams, 1996; Paoletti et al., 1997), we determined the effects of Zn^{2+} on agonist-induced currents of EGFP-NR1^{TCS}/NR2A-expressing oocytes before and after thrombin treatment (Fig. 2B). Recordings from untreated oocytes disclosed the typical biphasic Zn^{2+} inhibition curve with IC_{50} values of 0.028 ± 0.005 and 75 ± 8 μM for the high- and low-affinity Zn^{2+}-binding sites, respectively ($n = 5$). After a 1-h incubation with thrombin, the high-affinity component of

Zn^{2+} inhibition was reduced by >80%, with low-affinity Zn^{2+} inhibition predominating (259 ± 64 μM, n = 5; Fig. 2B right). In conclusion, thrombin efficiently cleaves surface-localized EGFP-$NR1^{TCS}$ subunits and thereby strongly reduces the affinity of Zn^{2+} inhibition at both NR1/NR2A and NR1/NR2B receptors.

N-Terminally Truncated NR1 Subunits Assembled Efficiently into Functional NMDA Receptors. To investigate the importance of the NR1-NTD for receptor assembly, we examined whether an N-terminally truncated NR1 subunit that lacks amino acids 5 to 358 of the mature NR1 subunit ($NR1^{\Delta NTD}$, Fig. 1A) forms heteromeric NMDA receptors after heterologous expression in *X. laevis* oocytes. To this end, we coexpressed the wt and the $NR1^{\Delta NTD}$ construct with the tagged NR2A*-His subunit (Madry et al., 2007) in oocytes that were metabolically labeled with [^{35}S]methionine. The NR2A*-His subunit was then purified under nondenaturating conditions by metal affinity chromatography from digitonin extracts of the oocytes and analyzed by reducing SDS-PAGE and autoradiography (Sadtler et al., 2003). Figure 3A, lane 1, shows that two ^{35}S-labeled bands with apparent molecular masses of approximately 116 and 105 kDa corresponding to those of the NR1 and NR2A*-His subunits, respectively, were coisolated by this protocol. Likewise, coexpression of the $NR1^{\Delta NTD}$ with the NR2A*-His construct resulted in coisolation of two ^{35}S-labeled bands with molecular masses of approximately 78 and 105 kDa, showing that the $NR1^{\Delta NTD}$ subunit also assembles with NR2A*-His (Fig. 3A, lane 2). Quantification of the subunit bands by PhosphorImaging revealed a ratio of ^{35}S-radioactivities of the wt NR1 subunit to the NR2A*-His polypeptide of 1.09 ± 0.16 (n = 3). This value is in good agreement with the theoretical ratio of 0.93, calculated from the determined subunit stoichiometry of 2NR1:2NR2 (Laube et al., 1998) and the known numbers of 28 and 30 methionine residues per mature NR1 and NR2A*-His subunit, respectively. Analysis of $NR1^{\Delta NTD}$/NR2A*-His receptors yielded a ratio of 0.60 ± 0.09 (n = 3) of $NR1^{\Delta NTD}$ to NR2A* subunit radioactivities. This is consistent with a lower number (18) of methionine residues in $NR1^{\Delta NTD}$, which predicts a theoretical ratio of 0.60 for a receptor complex containing two $NR1^{\Delta NTD}$ and two NR2A*-His subunits. Because the intensities of the NR2A*-His polypeptide bands were not different in the affinity-purified NR1/NR2A*-His and $NR1^{\Delta NTD}$/NR2A*-His receptors, the values obtained for both preparations, at the close-to-theoretical NR1/NR2A ratio of 1:1, indicate that 1) both the wt NR1 and $NR1^{\Delta NTD}$ subunits assemble at a 2:2 stoichiometry with NR2A*-His, and 2) both NR1 polypeptides show comparable assembly efficiencies. In conclusion, NMDA receptor formation seems not to depend on the NTD of the NR1 subunit.

NTD-Deleted NR1 and NR2 Subunits Generated Functional NMDA Receptors. A previous study has shown that coexpression of NTD-deleted NR2A and NR2B subunits with wt NR1 generates functional NMDA receptors (Paoletti et al., 2000). To analyze whether the NTD deleted NR1 subunit $NR1^{\Delta NTD}$ assembles into functional receptors upon coexpression with the NR2A or NR2B subunit, we applied saturating glutamate and glycine concentrations (100 μM each) to recombinant NR1/NR2B, $NR1^{\Delta NTD}$/NR2B, NR1/$NR2B^{\Delta NTD}$, and $NR1^{\Delta NTD}$/$NR2B^{\Delta NTD}$ receptors. All subunit combinations mentioned above were found to produce robust currents with I_{max} values that were not significantly different from each other (Fig. 3B; Tables 1 and 2). Likewise, receptors composed of NTD-deleted NR1 and NR2A subunits displayed robust agonist responses in the presence of saturating agonist concentrations, with I_{max} values similar to those of wt NR1/NR2A receptors (Table 1). Furthermore, we determined the extent of current decay of NR1/NR2A-, NR1NR2B-, $NR1^{\Delta NTD}$/$NR2A^{\Delta NTD}$-, and $NR1^{\Delta NTD}$/$NR2B^{\Delta NTD}$-expressing oocytes in the continuous presence of saturating glycine and glutamate concentrations (100 μM each) by measuring the ratio of the peak (I_p) and steady-state (I_{ss}) current as an estimate for receptor desensitization. Figure 3C, left, shows typical traces recorded from wt NR1/NR2A and mutant $NR1^{\Delta NTD}$/$NR2A^{\Delta NTD}$ receptors, which rapidly reached peak amplitude and then strongly decayed to steady-state currents in the presence of agonists. For wt NR1/NR2A channels, the

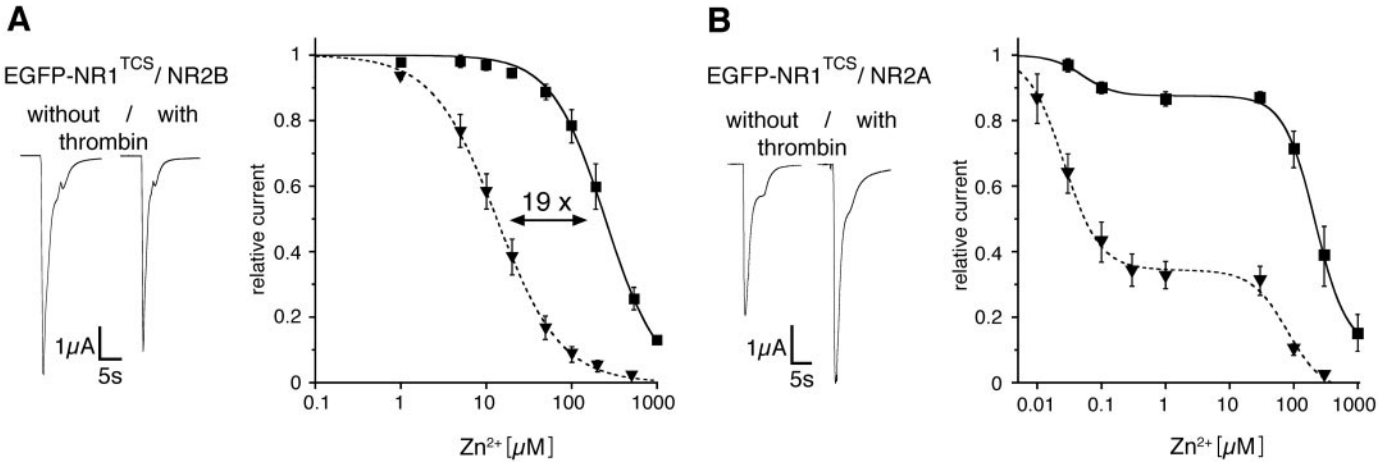

Fig. 2. Functional characterization of $NR1^{TCS}$/NR2A and $NR1^{TCS}$/NR2B receptors before and after thrombin cleavage. Dose-response analysis of receptors formed by the EGFP-$NR1^{TCS}$ subunit upon coexpression with either the NR2B (A) or the NR2A (B) subunits in *X. laevis* oocytes before (▼, broken line) and after (■, full line) thrombin treatment by two-electrode voltage clamping. Left, comparison of agonist-induced currents of EGFP-$NR1^{TCS}$/NR2A and -NR2B-expressing cells elicited by application of glutamate and glycine (100 μM, each) before and after a 1-h exposure to thrombin. Right, Zn^{2+} inhibition curves determined before and after thrombin cleavage revealed an approximately 19-fold reduction in the apparent Zn^{2+} affinity of EGFP-$NR1^{TCS}$/NR2B (A) receptors and an almost complete loss of high-affinity Zn^{2+} inhibition for EGFP-$NR1^{TCS}$/NR2A (B) receptors upon proteolytic cleavage of the NR1 NTD.

extent of desensitization expressed as a percentage of the peak current was 83 ± 2.4% (n = 13), whereas mutant receptors showed a significantly decreased extent of desensitization (51 ± 1.3%; n = 13) (Fig. 3D). Analysis of wt NR1/NR2B and mutant NR1$^{\Delta NTD}$/NR2B$^{\Delta NTD}$ receptors revealed no differences in the desensitization ratios with values of 54 ± 1.2 and 54 ± 5.5% (n = 13), respectively (Fig. 3, C, right traces, and D). Overall, these data clearly show that the NTDs of the NR1 and NR2 subunits are not required for NMDA receptor assembly and membrane insertion but may play a role in determining receptor-kinetics.

The NR1-NTD Was Required for High-Affinity Zn^{2+} Inhibition of NR1/NR2A Receptors. The NTD of the NR2A subunit is known to harbor crucial determinants of the voltage-independent, high-affinity inhibition by Zn^{2+} (Choi and Lipton, 1999; Fayyazuddin et al., 2000; Paoletti et al.,

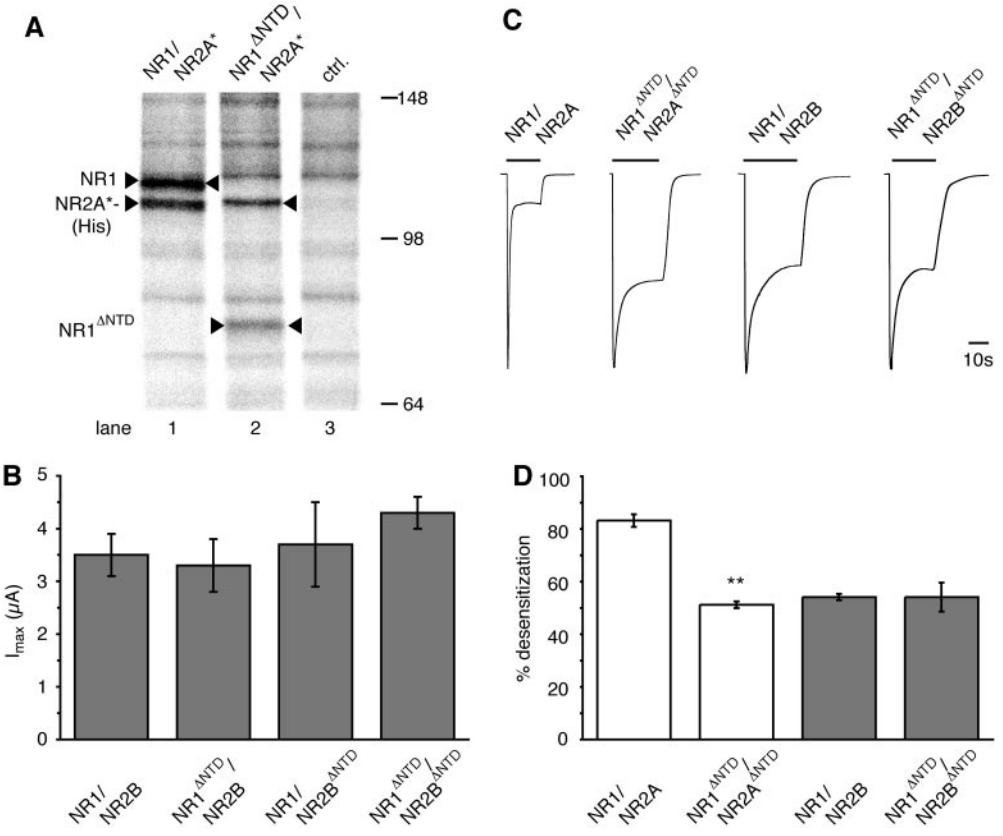

Fig. 3. Assembly and functional properties of NMDA receptors containing NTD-deleted NR1 and/or NR2 subunits. A, the NR1$^{\Delta NTD}$ subunit forms hetero-oligomers with the NR2A subunit. *X. laevis* oocytes coexpressing a His-tagged NR2A* with nontagged NR1 or NR1$^{\Delta NTD}$ subunits were metabolically labeled with [^{35}S]methionine, and the receptor complexes formed were isolated by affinity purification and analyzed by SDS-PAGE. Lane 1 shows two bands with apparent molecular masses of approximately 116 and 105 kDa, which represent the coisolated wt NR1 and NR2A*-His subunits. Coexpression of the NR1$^{\Delta NTD}$ with the NR2A*-His construct similarly resulted in coisolation of two ^{35}S-labeled bands with molecular masses of approximately 78 and 105 kDa, which correspond to the NR1$^{\Delta NTD}$ and NR2A*-His subunits (lane 2). Lane 3, isolate from noninjected oocytes. B, quantitative analysis of wt NR1/NR2B-, NR1$^{\Delta NTD}$/NR2B-, NR1/NR2B$^{\Delta NTD}$-, and NR1$^{\Delta NTD}$/NR2B$^{\Delta NTD}$-expressing oocytes showed no significant differences in the mean maximal agonist-inducible whole-cell currents (1 s application of 100 μM glutamate and glycine, each) compared with wt NR1/NR2B receptors (Table 2). C, examples of current traces showing the extent of desensitization of NR1/NR2A, NR1$^{\Delta NTD}$/NR2A$^{\Delta NTD}$, NR1/NR2B, and NR1$^{\Delta NTD}$/NR2B$^{\Delta NTD}$ receptor combinations to sustained application of glutamate and glycine (100 μM, each). D, relative ratios of steady-state (I_{ss}) versus peak (I_p) currents of NR1/NR2A, NR1/NR2B, NR1$^{\Delta NTD}$/NR2A$^{\Delta NTD}$, and NR1$^{\Delta NTD}$/NR2B$^{\Delta NTD}$ receptors. Note a significant decrease in the extent of receptor desensitization (%) for the NR1$^{\Delta NTD}$/NR2A$^{\Delta NTD}$ combination compared with wt.

TABLE 1

Pharmacology of NMDA receptors assembled from wt and NTD-deleted NR1/NR2A subunits

Glycine and glutamate EC_{50} values were determined in the presence of 100 μM glutamate or glycine, respectively. IC_{50} values of Zn^{2+} were obtained by preincubating the cells with the allosteric inhibitor followed by coapplying the inhibitor with 100 μM each glutamate and glycine. cRNAs were injected at a NR1/NR2 ratio of 1:2, and recordings were performed after 2 to 3 days of expression. Values represent means ± S.E. Number of experiments was between 5 and 21.

Subunit Composition	I_{max}	EC_{50}		IC_{50} Zn^{2+}	
		Glu	Gly	High Affinity	Low Affinity
	μA	μM		μM	
NR1/NR2A	5.4 ± 0.3	2.6 ± 0.4	1.7 ± 0.2	0.012 ± 0.004	225 ± 19
NR1$^{\Delta NTD}$/NR2A	8.5 ± 1.0	1.7 ± 0.3	1.8 ± 0.2	N.D.	305 ± 79
NR1/NR2A$^{\Delta NTD}$	5.0 ± 1.9	3.6 ± 0.7	2.1 ± 0.4	N.D.	319 ± 99
NR1$^{\Delta NTD}$/NR2A$^{\Delta NTD}$	6.4 ± 0.8	4.6 ± 1.1	2.7 ± 0.5	N.D.	302 ± 61

N.D., not detectable.

2000). Recordings of wt NR1/NR2A receptors exhibited a biphasic Zn^{2+} inhibition-response curve, with IC_{50} values in the nanomolar and micromolar ranges (Table 1) and a maximal inhibition of approximately 60% exerted via the high-affinity site (Fig. 4A). To examine whether coassembly with the $NR1^{\Delta NTD}$ construct would result in a similar reduction of Zn^{2+} inhibition as seen upon thrombin treatment of $NR1^{TCS}$/NR2A receptors, we coexpressed different combinations of wt and NTD-deleted NR1 and NR2A subunits. With the $NR1^{\Delta NTD}$/NR2A, NR1/$NR2A^{\Delta NTD}$, and $NR1^{\Delta NTD}$/$NR2A^{\Delta NTD}$ combinations, we found a complete loss of high-affinity Zn^{2+} inhibition; only a low-affinity inhibitory component persisted at all these truncated receptors (Fig. 4A, Table 1). Thus, not only the NR2A-NTD but also the NR1-NTD are crucially required for high-affinity Zn^{2+} inhibition of NR1/NR2A receptors.

Both NR1- and NR2B-NTDs Contributed to Zn^{2+} and Ifenprodil Inhibition. To unravel possible roles of the NTDs also in NR1/NR2B receptor modulation, we first analyzed the effects of Zn^{2+} on all possible combinations of wt and NTD-deleted NR1 and NR2B subunits (i.e., NR1/NR2B, $NR1^{\Delta NTD}$/NR2B, NR1/$NR2B^{\Delta NTD}$, and $NR1^{\Delta NTD}$/$NR2B^{\Delta NTD}$). Analysis of the respective inhibition curves revealed significant differences in Zn^{2+} sensitivity (Table 2). Both single and double deletions of the NTDs of the NR1 and/or NR2B subunits markedly increased to a similar extent the concentration of Zn^{2+} required to half-maximally inhibit NR1/NR2B receptors (Fig. 4B; Table 2). We furthermore examined the role of the NTDs for inhibition by the synthetic neuroprotective compound ifenprodil, which has been reported to allosterically inhibit NMDA receptors via the NTD of the NR2B subunit (Perin-Dureau et al., 2002). At wt NR1/NR2B receptors, ifenprodil displayed an IC_{50} value of 0.89 ± 0.08 μM (Fig. 4C). Again, single as well as double deletions of the NTDs of NR1 and NR2B subunits caused a >100-fold reduction in inhibitory potency (Fig. 4C, Table 2). Overall, our data emphasize the importance of both the NR1- and NR2-NTDs for high-affinity allosteric Zn^{2+} and ifenprodil inhibition of NR1/NR2A and NR1/NR2B receptors.

Residual Zn^{2+} and Ifenprodil Inhibition of NTD-Deleted Receptors Was Mediated by Both Voltage-Dependent and -Independent Low-Affinity Components. To reveal whether the residual low-affinity Zn^{2+}- and ifenprodil inhibition seen with NTD-deleted NR1/NR2B receptors (see Table 2) is mediated by either a channel-blocking effect or a voltage-independent low-affinity site, we analyzed the current-voltage relationship of agonist currents recorded in the presence of Zn^{2+}. Whereas in Mg^{2+}-free medium, the current-voltage relation of wt NR1/NR2B receptors was linear in the presence of 10 μM Zn^{2+} (Fig. 5A), the inhibition of NTD-deleted $NR1^{\Delta NTD}$/NR2B, NR1/$NR2B^{\Delta NTD}$, and $NR1^{\Delta NTD}$/$NR2B^{\Delta NTD}$ receptors seen in the presence of 100 μM Zn^{2+} was found to be composed of a voltage-dependent and -independent component (Fig. 5, B–D). The latter, detected at positive holding potentials, is likely mediated via a separate Zn^{2+} binding site located within domains distinct from the NTDs (see Fayyazuddin et al., 2000; Rachline et al., 2005). Similar to Zn^{2+} inhibition, the remaining ifenprodil effect observed with the NTD-deleted receptors displayed voltage dependence at negative holding potentials (not shown). We therefore conclude that, besides a voltage-dependent channel block, NR1/NR2A and NR1/NR2B receptors harbor a common voltage-independent Zn^{2+}-binding site outside the NTDs responsible for voltage-independent low-affinity Zn^{2+} inhibition.

Removal of NR1- and/or NR2B-NTDs Reduced Glycine Affinity. We initially observed that thrombin cleavage of EGFP-$NR1^{TCS}$/NR2B receptors reduced not only their Zn^{2+} sensitivity but also increased the EC_{50} value of glycine (0.30 ± 0.04 versus 0.80 ± 0.14 μM). This prompted us to determine the apparent glutamate and glycine affinities of NTD-deleted NR1/NR2A and NR1/NR2B receptors. In agreement with previous studies (Laurie and Seeburg, 1994; Priestley et al., 1995), the glycine affinities of NR1/NR2A and NR1/NR2B receptors were found to be significantly different (Fig. 6A), with EC_{50} values of 1.7 ± 0.2 versus 0.39 ± 0.04 μM, respectively ($p < 0.001$; Tables 1 and 2). We saw significant changes in glycine EC_{50} values only with NTD-deleted NR1/NR2B receptor combinations (Fig. 6B, Tables 1 and 2), whereas the glycine affinity of NR2A-containing receptors remained unaltered upon NTD removal (Fig. 6B, Table 1). No changes in glutamate affinities were obtained for either NR1/NR2A or NR1/NR2B receptors after NTD-deletion (Tables 1 and 2). Hence, both the NR1- and the NR2B-NTDs are essential for high-affinity glycine binding to NR1/NR2B receptors.

To further examine whether the NR2-NTDs play a role in determining the different glycine affinities of distinct NMDA receptor subtypes, we used two chimeric constructs in which the NTD of NR2A was replaced by the corresponding NR2B-NTD ($NR2A^{NTD2B}$), and vice versa ($NR2B^{NTD2A}$), as detailed previously (Paoletti et al., 2000). NR1/$NR2A^{NTD2B}$ receptors were found to have the same glycine EC_{50} value as wt NR1/NR2B receptors (Fig. 6, A and B; 0.28 ± 0.09 versus 0.39 ± 0.04 μM; $p > 0.05$, $n = 4$), which was significantly different from the EC_{50} value of the wt NR1/NR2A receptor ($p < 0.01$, $n = 5$). Inversely, NR1/$NR2B^{NTD2A}$ receptors displayed an

TABLE 2

Pharmacology of NMDA receptors assembled from wt and NTD-deleted NR1/NR2B subunits

Glycine and glutamate EC_{50} values were determined in the presence of 100 μM glutamate or glycine, respectively. IC_{50} values of Zn^{2+} and ifenprodil were obtained by preincubating the cells with the allosteric inhibitor followed by coapplying the inhibitor with 100 μM each glutamate and glycine. cRNAs were injected at a NR1/NR2 ratio of 1:2, and recordings were performed after 2 to 3 days of expression. Values represent means ± S.E. Number of experiments was between 5 and 21.

Subunit Composition	I_{max}	EC_{50}		IC_{50}	
		Glu	Gly	Zn^{2+}	Ifenprodil
	μA	μM		μM	
NR1/NR2B	3.5 ± 0.4	1.8 ± 0.4	0.39 ± 0.04	6.8 ± 1.7	0.89 ± 0.08
$NR1^{\Delta NTD}$/NR2B	3.3 ± 0.5	4.0 ± 1.0	6.6 ± 1.6**	51 ± 7**	129 ± 14**
NR1/$NR2B^{\Delta NTD}$	3.7 ± 0.8	0.95 ± 0.1	1.8 ± 0.1**	37 ± 3**	140 ± 14**
$NR1^{\Delta NTD}$/$NR2B^{\Delta NTD}$	4.3 ± 0.3	2.3 ± 0.4	2.8 ± 0.6*	126 ± 29**	124 ± 29**

* $P < 0.01$.
** $P < 0.001$.

apparent glycine affinity indistinguishable from that of wt NR1/NR2A receptors (Fig. 6, A and B; 2.4 ± 0.4 versus 1.7 ± 0.3 μM, $p > 0.05$, $n = 3$). In contrast, no significant differences in glutamate affinities between wt NR1/NR2A and NR1/NR2B receptors and the respective chimeric receptors were observed (Fig. 6C). Thus, the NTDs of NR2A and NR2B determine not only allosteric inhibition but also the glycine affinity of different NMDA receptor subtypes.

Discussion

In this article, we examined the contributions of the N-terminal LIVBP-homology domains of the NR1 and the NR2 subunits to NMDA receptor assembly, function, and allosteric inhibition. We showed that the NTDs are not required for subunit assembly and channel function. However, high-affinity inhibition by Zn^{2+} or ifenprodil was abolished upon NTD deletion of either the NR1 or NR2 subunit, indicating that both NTDs are required for allosteric receptor inhibition. Furthermore, the different apparent glycine affinities of NR1/NR2A versus NR1/NR2B receptors were found to be determined by their respective NR2-NTDs.

Role of the NTDs in NMDA Receptor Modulation. Several studies have shown that the LIVBP-like domains in both ionotropic and metabotropic GluRs are capable of specifically forming dimers or higher-order oligomers via interdomain interactions (Kuusinen et al., 1999; Kunishima et al., 2000). In non-NMDA receptors of the iGluR family, these interactions have been implicated in subunit assembly (Ayalon and Stern-Bach, 2001; Matsuda et al., 2005). Here, we show that NTD-deleted NMDA receptor subunits form functional channels with agonist-induced currents similar to those of wt receptors; this clearly excludes an essential role of the NTDs in the assembly of NR1/NR2 receptors. This finding is consistent with the data obtained by others (Fayyazuddin et al., 2000; Hu and Zheng, 2005), where deletion of the NR2 NTDs resulted in functional NMDA receptors. However, Meddows et al. (2001) reported that deletion of the first 380 amino acid residues of the NR1 subunit impairs subunit oligomerization. We attribute this different result to the longer deletion used by these authors than that studied here. Our data are also in agreement with studies obtained for other members of the iGluR family, which demonstrate proper assembly of natural and recombinant subunits lacking an NTD (Chen et al., 1999; Pasternack et al., 2002).

Although interactions between the NTDs of the NMDA receptor subunits are not required for receptor assembly, both thrombin-mediated cleavage of the NR1-NTD and deletion of the NR1- or NR2-NTDs abrogated voltage-independent high-affinity Zn^{2+} and ifenprodil inhibition. This clearly demonstrates that the NR1-NTD is required for the inhibitory effects exerted by these allosteric inhibitors, although both have shown to bind to the NR2-NTDs (overview in Herin and Aizenman, 2004). The residual low-affinity voltage-independent and -dependent inhibition observed upon NTD deletion are probably due to additional binding sites located outside the NTDs and within the channel region, respectively (Paoletti et al., 1997, Traynelis et al., 1998; Rachline et al., 2005).

Model of NTD-Mediated Inhibition. Previous studies indicate that both ifenprodil and Zn^{2+} share common binding sites and mechanisms, which result in increased NMDA receptor desensitization upon binding-induced domain closure of the LIVBP-homology region (Chen et al., 1997; Paoletti et al., 1997, 2000; Krupp et al., 1998; Low et al., 2000; Zheng et al., 2001). This is also consistent with our finding that removal of the NTDs of the NR1/NR2A receptor slows receptor desensitization. Based on these data, we favor a mechanism of NTD-mediated NMDA receptor inhibition that is adapted from a recent model of AMPA receptor activation (Mayer, 2006) and relies on 1) the crystallographically demonstrated heterodimeric arrangement of NR1 and NR2 subunits (Furukawa et al., 2005) and 2) iGluR desensitization resulting from a disruption of LBD interdomain-interactions (Armstrong et al., 2006). Accordingly, binding of an allosteric inhibitor to the NR2-NTD is proposed to induce closure of the LIVBP-homology domain and to thereby produce a conformational strain, which weakens interdomain interactions be-

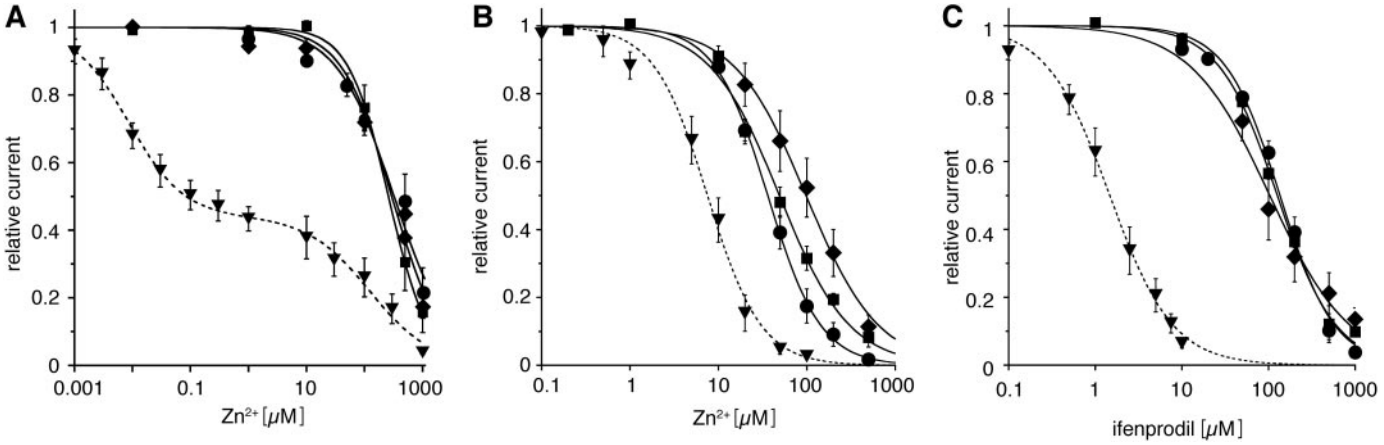

Fig. 4. Allosteric inhibition by Zn^{2+} and ifenprodil of NMDA receptors containing NTD-deleted NR1 and/or NR2 subunits. A and B, inhibition of agonist-evoked currents by Zn^{2+} at wt and NTD-deleted NR1/NR2 receptors. Agonist concentrations were 100 μM glycine and glutamate, each. A, Zn^{2+} inhibition of wt NR1/NR2A (▼), $NR1^{\Delta NTD}$/NR2A (■), NR1/$NR2A^{\Delta NTD}$ (●), and $NR1^{\Delta NTD}$/$NR2A^{\Delta NTD}$ (♦) receptors. Note biphasic inhibition of the wt receptor, with high (HA) and low-affinity (LA) sites displaying IC_{50} values of 0.012 ± 0.004 μM (60% inhibition) and 225 ± 19 μM (40% inhibition), respectively. HA Zn^{2+}-inhibition was eliminated in all mutant combinations, whereas LA inhibition was not affected. B, Zn^{2+} inhibition of wt NR1/NR2B (▼), $NR1^{\Delta NTD}$/NR2B (■), NR1/$NR2B^{\Delta NTD}$ (●), and $NR1^{\Delta NTD}$/$NR2B^{\Delta NTD}$ (♦) receptors. C, ifenprodil inhibition of the NR1/NR2B receptor combinations described under (B). Note similar residual inhibition of $NR1^{\Delta NTD}$/NR2B, NR1/$NR2B^{\Delta NTD}$, and $NR1^{\Delta NTD}$/$NR2B^{\Delta NTD}$ receptors for Zn^{2+} and ifenprodil. For IC_{50} values, see Tables 1 and 2.

tween NR1- and NR2-LBDs (Fig. 7). This facilitates receptor desensitization upon agonist binding. An important feature of our model is that only binding of an allosteric modulator to an NR2-NTD stabilized by an adjacent NR1-NTD would be able to sufficiently weaken the interactions between NR1 and NR2 LBDs (Fig. 7) (Armstrong et al., 2006). This implies that the NR1 and NR2 LIVBP homology domains form a heterodimer, an idea that is entirely consistent with both the heterodimeric arrangement of NR1 and NR2 subunits (Furukawa et al., 2005) and our data showing that both the NR1 and NR2 NTDs equally contribute to high-affinity Zn^{2+} and ifenprodil inhibition. Our model assigning an important role to the NTD heterodimer (Fig. 7) is also consistent with the observation that the glycine affinity of NMDA receptors containing chimeric NR2 subunits is determined by their respective NR2-NTDs.

Contribution of NTDs in Determining Agonist Affinity. The pharmacological profile of NMDA receptors is known to crucially depend on the NR2 subunit isoform incorporated (Laurie and Seeburg, 1994; overview in Cull-Candy et al., 2001). For example, NR1/NR2B receptors have a 10-fold higher glycine affinity than NR1/NR2A receptors (Laurie and Seeburg, 1994; Priestley et al., 1995; current study), although both receptors share the same glycine-binding NR1 subunit. Here, we showed that upon coexpression with NR1, a chimeric NR2A subunit containing the NTD of NR2B generates receptors displaying the high glycine affinity characteristic of wt NR1/NR2B receptors. Vice versa, the EC_{50} value of glycine at NR1/NR2B^{NTD2A} receptors was similar to that determined for wt NR1/NR2A receptors. These results are consistent with the observation that mutations within NR2-NTDs can affect apparent glycine affinity (Choi et al., 2001). All these findings can be explained by allosteric interactions between the NTDs of the NMDA receptor subunits, which determine both the affinity of glycine binding to the

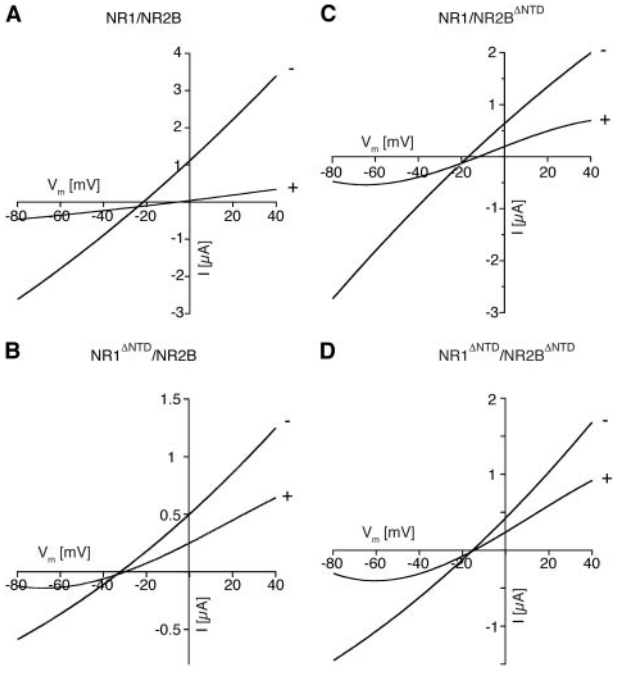

Fig. 5. Effect of the NTD-deletions of the NR1 and/or NR2B subunits on the voltage dependence of Zn^{2+} inhibition. Current-voltage (I-V) relationships for oocytes expressing wt NR1/NR2B (A), NR1$^{\Delta NTD}$/NR2B (B), NR1/NR2B$^{\Delta NTD}$ (C), and NR1$^{\Delta NTD}$/NR2B$^{\Delta NTD}$ (D) receptors in the absence (−) and presence (+) of Zn^{2+} at the respective IC_{50} value (see Table 2). Note that current-voltage curves for wt NR1/NR2B (A) receptors in the presence of 10 μM Zn^{2+} exhibit only a high-affinity voltage-independent inhibition, whereas NR1$^{\Delta NTD}$/NR2B (B), NR1/NR2B$^{\Delta NTD}$ (C) and NR1$^{\Delta NTD}$/NR2B$^{\Delta NTD}$ (D) receptors display a combination of a low-affinity voltage-independent and -dependent inhibition in the presence of 100 μM Zn^{2+}.

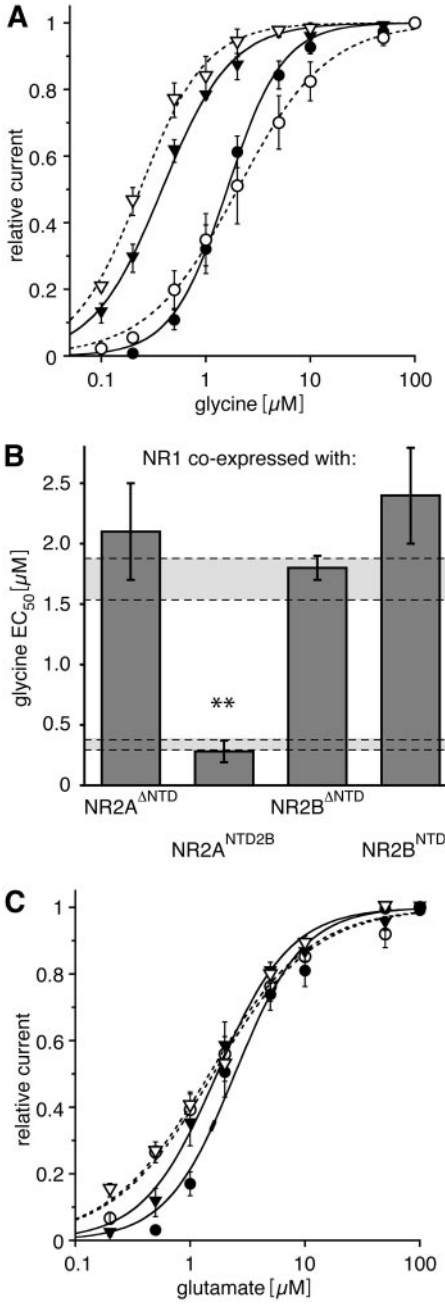

Fig. 6. Agonist response properties of NMDA receptors containing N-terminally deleted and chimeric NR2A or NR2B subunits. A, dose-response curves for glycine determined in the presence of saturating concentrations of glutamate (100 μM) at wt NR1/NR2A (●, 1.7 ± 0.3 μM) and NR1/NR2B (▼, 0.39 ± 0.04 μM), and at chimeric NR1/NR2A^{NTD2B} (▽, 0.28 ± 0.09 μM) and NR1/NR2B^{NTD2A} (○, 2.4 ± 0.9 μM) receptors. B, comparison of the glycine EC_{50} values of NR1/NR2 receptors containing NTD-deleted and chimeric NR2 subunits compared with the respective wt proteins. Apparent glycine affinities of wt NR1/NR2A and NR1/NR2B receptors (± S.E.) are indicated by dotted lines. C, dose-response curves for glutamate determined in the presence of saturating concentrations of glycine (100 μM) for NR1/NR2A (●, 2.6 ± 0.4 μM), NR1/NR2B (▼, 1.8 ± 0.4 μM), NR1/NR2A^{NTD2B} (▽, 2.0 ± 0.3 μM), and NR1/NR2B^{NTD2A} (○, 1.6 ± 0.5 μM) receptors.

NR1 subunit and the efficacy of allosteric inhibitors at the NR2 subunits.

Implications for the Pathology and Therapy of t-PA-Triggered Neurotoxicity. Excessive stimulation of NMDA receptors is known to cause neuronal cell death by apoptosis or necrosis as a result of enhanced Ca^{2+} influx (overview in Cull-Candy et al., 2001). NMDA receptors are tonically inhibited by Zn^{2+}, a mechanism that has been shown to protect neurons against NMDA receptor-mediated glutamate toxicity in vitro (Chen et al., 1997). Here, we demonstrate that deletion of the NR1-NTD by thrombin abolishes high-affinity Zn^{2+} inhibition of NR1/NR2A receptors. Tissue-type plasminogen activator (t-PA), an endogenous serine protease, has been found to potentiate NMDA receptor currents through cleavage of the NR1-NTD, which has been implicated in pathophysiological aspects of glutamatergic neurotransmission (Nicole et al., 2001; Fernández-Monreal et al., 2004). After focal cerebral ischemia, t-PA triggers the neurotoxic cascade mediated by elevated concentrations of glutamate (Tsirka et al., 1995). Blockade of this serine protease in cortical neuron cultures has been reported to reduce NMDA-induced excitotoxic cell death (Nicole et al., 2001). Because we found a loss in Zn^{2+} inhibition of both NR1/NR2A and NR1/NR2B receptors upon thrombin cleavage and deletion of the NR1-NTD, our results might provide an explanation for the enhanced NMDA receptor activity seen in the presence of t-PA. Accordingly, relief of NMDA receptors from tonic Zn^{2+} inhibition (Rachline et al., 2005) by t-PA-mediated cleavage of the NR1-NTD would result in enhanced Ca^{2+} influx and thereby cause neuronal cell death. This mechanism should be particularly effective at synaptically localized NR1/NR2A receptors, as a result of their high-affinity Zn^{2+}-binding site.

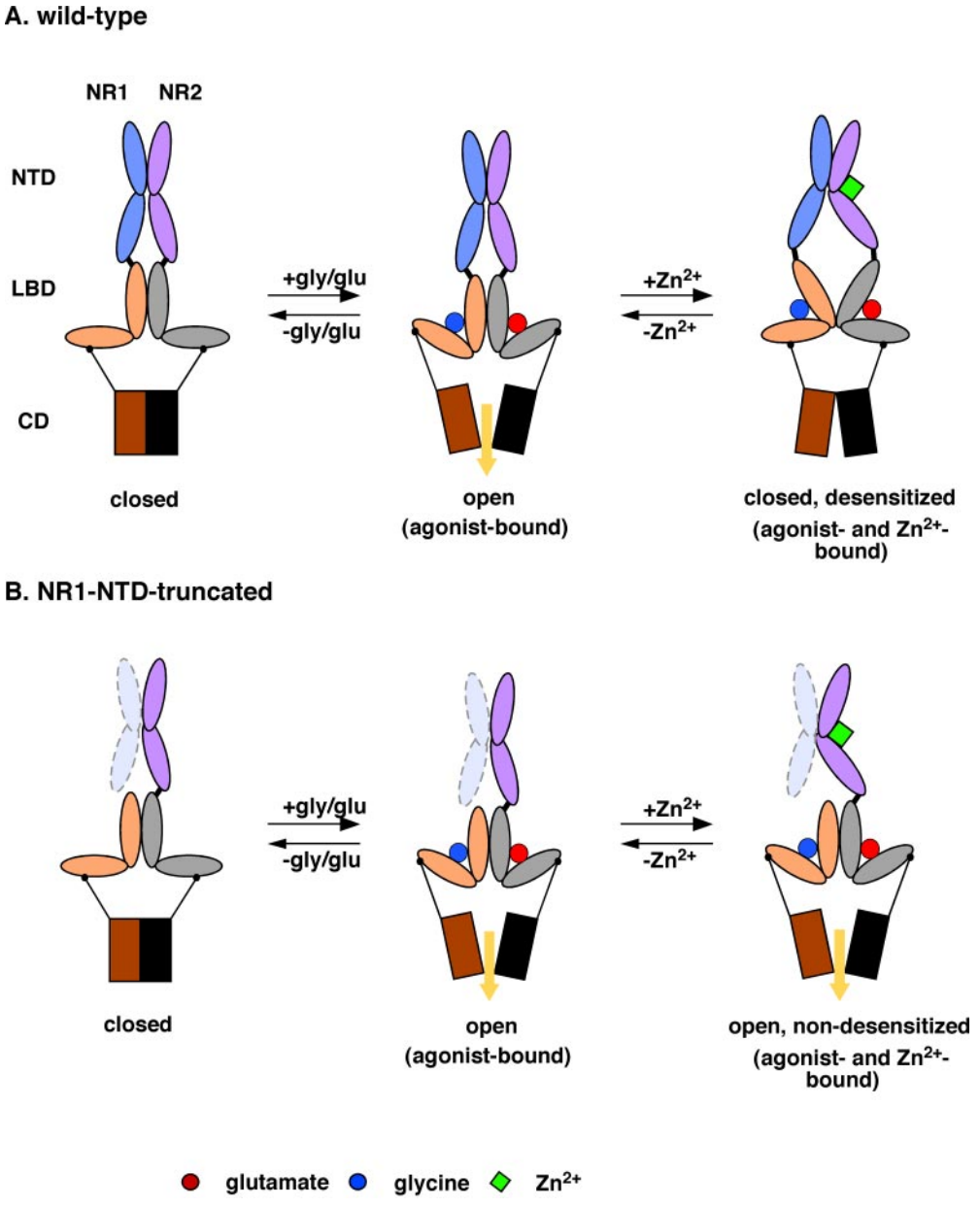

Fig. 7. Model illustrating the conformational changes proposed to occur upon Zn^{2+} or ifenprodil binding to wt and NTD-deleted NMDA receptors. Binding of Zn^{2+} or ifenprodil to the open, agonist-bound ion channel is thought to cause a closure of the NR2-NTD. This results in weakening of NR1-NR2-LBD interactions and thereby promotes closure of the channel by enhanced desensitization (see Armstrong et al., 2006). For simplicity, only one NR1-NR2 dimer of the tetrameric receptor is shown. NTD, N-terminal domain; LBD, ligand-binding domain; CD, channel domain. Yellow arrow indicates ion flux through the open channel. A, gating scheme for the wt NR1/NR2 receptor showing the heterodimeric organization of the LBDs and the NTDs of the NR1 and NR2 subunits (left, closed unliganded receptor). Binding of glycine (blue circle) to the NR1-LBD and of glutamate (red circle) to the NR2-LBD results in channel opening (middle). Weakening of NR1-NR2-LBD interactions by binding of Zn^{2+} (green rectangle) or ifenprodil to the respective NR2-NTD leads to a conformational strain, which disrupts the LBD interface and thus drives the receptor into the desensitized closed state (right). B, reaction scheme for the NR1-NTD-truncated receptor. Here, deletion or enzymatic cleavage of the NR1-NTD results in a loss of conformational strain deriving from Zn^{2+} binding, and thereby prevents weakening of LBD interactions. Consequently, the Zn^{2+} occupied receptors resides in its open state. The truncated NR1-NTD still associated with the "core" receptor after thrombin cleavage is indicated by lucent drawing.

Acknowledgments

We thank Dr. P. Paoletti for providing the NR2A$^{\Delta NTD}$, NR2B$^{\Delta NTD}$, NR2B^{NTD2A}, and NR2A^{NTD2B} cDNAs, Dr. A. Nicke for technical advice on metabolic labeling, and Drs. J. R. P. Geiger and B. Mathias-Costa for critical reading of the manuscript.

References

Armstrong N, Jasti J, Beich-Frandsen M, and Gouaux E (2006) Measurement of conformational changes accompanying desensitization in an ionotropic glutamate receptor. *Cell* **127:**85–97.

Ayalon G and Stern-Bach Y (2001) Functional assembly of AMPA and kainate receptors is mediated by several discrete protein-protein interactions. *Neuron* **31:**103–113.

Chen GQ, Cui C, Mayer ML, and Gouaux E (1999) Functional characterization of a potassium-selective prokaryotic glutamate receptor. *Nature* **402:**817–821.

Chen N, Moshaver A, and Raymond LA (1997) Differential sensitivity of recombinant *N*-methyl-D-aspartate receptor subtypes to zinc inhibition. *Mol Pharmacol* **51:**1015–1023.

Choi YB, Chen HS, and Lipton SA (2001) Three pairs of cysteine residues mediate both redox and Zn^{2+} modulation of the NMDA receptor. *J Neurosci* **21:**392–400.

Choi YB and Lipton SA (1999) Identification and mechanism of action of two histidine residues underlying high-affinity Zn^{2+} inhibition of the NMDA receptor. *Neuron* **23:**171–180.

Cull-Candy S, Brickley S, and Farrant M (2001) NMDA receptor subunits: diversity, development and disease. *Curr Opin Neurobiol* **11:**327–335.

Dingledine R, Borges K, Bowie D, and Traynelis SF (1999) The glutamate receptor ion channels. *Pharmacol Rev* **51:**7–61.

Fayyazuddin A, Villarroel A, Le Goff A, Lerma J, and Neyton J (2000) Four residues of the extracellular N-terminal domain of the NR2A subunit control high-affinity Zn^{2+} binding to NMDA receptors. *Neuron* **25:**683–694.

Fernández-Monreal M, López-Atalaya J, Benchenane K, Cacquevel M, Dulin F, Le Caer JP, Rossier J, Jarrige AC, MacKenzie E, Colloc'h N, et al. (2004) Arginine 260 of the amino-terminal domain of the NR1 subunit is critical for tissue-type plasminogen activator-mediated enhancement of *N*-methyl-D-aspartate receptor signalling. *J Biol Chem* **279:**50850–50856.

Furukawa H, Singh SK, Mancusso R, and Gouaux E (2005) Subunit arrangement and function in NMDA receptors. *Nature* **438:**185–192.

Herin GA and Aizenman E (2004) Amino-terminal domain regulation of NMDA receptor function. *Eur J Pharmacol* **500:**101–111.

Hu B and Zheng F (2005) Molecular determinants of glycine-independent desensitization of NR1/NR2A receptors. *J Pharmacol Exp Ther* **313:**563–569.

Krupp JJ, Vissel B, Heinemann SF, and Westbrook GL (1998) N-terminal domains in the NR2 subunit control desensitization of NMDA receptors. *Neuron* **20:**317–327.

Kunishima N, Shimada Y, Tsuji Y, Sato T, Yamamoto M, Kumasaka T, Nakanishi S, Jingami H, and Morikawa K (2000) Structural basis of glutamate recognition by a dimeric metabotropic glutamate receptor. *Nature* **407:**971–977.

Kuryatov A, Laube B, Betz H, and Kuhse J (1994) Mutational analysis of the glycine-binding site of the NMDA receptor: structural similarity with bacterial amino acid-binding proteins. *Neuron* **12:**1291–1300.

Kuusinen A, Abele R, Madden DR, and Keinanen K (1999) Oligomerization and ligand-binding properties of the ectodomain of the α-amino-3-hydroxy-5-methyl-4-isoxazole propionic acid receptor subunit GluRD. *J Biol Chem* **274:**28937–28943.

Laube B, Hirai H, Sturgess M, Betz H, and Kuhse J (1997) Molecular determinants of agonist discrimination by NMDA receptor subunits: analysis of the glutamate binding site on the NR2B subunit. *Neuron* **18:**493–503.

Laube B, Kuhse J, and Betz H (1998) Evidence for a tetrameric structure of recombinant NMDA receptors. *J Neurosci* **18:**2954–2961.

Laube B, Kuhse J, Rundstrom N, Kirsch J, Schmieden V, and Betz H (1995) Modulation by zinc ions of native rat and recombinant human inhibitory glycine receptors. *J Physiol* **483:**613–619.

Laurie DJ and Seeburg PH (1994) Ligand affinities at recombinant *N*-methyl-D-aspartate receptors depend on subunit composition. *Eur J Pharmacol* **268:**335–345.

Low CM, Zheng F, Lyuboslawsky P, and Traynelis SF (2000) Molecular determinants of coordinated proton and zinc inhibition of *N*-methyl-D-aspartate NR1/NR2A receptors. *Proc Natl Acad Sci U S A* **97:**11062–11067.

Madden DR (2002) The structure and function of glutamate receptor ion channels. *Nat Rev Neurosci* **3:**91–101.

Madry C, Mesic I, Bartholomäus I, Nicke A, Betz H, and Laube B (2007) Principal role of NR3 subunits in NR1/NR3 excitatory glycine receptor function. *Biochem Biophys Res Commun* **354:**102–108.

Matsuda S, Kamiya Y, and Yuzaki M (2005) Roles of the N-terminal domain on the function and quaternary structure of the ionotropic glutamate receptor. *J Biol Chem* **280:**20021–20029.

Mayer ML (2006) Glutamate receptors at atomic resolution. *Nature* **440:**456–462.

Meddows E, Le Bourdelles B, Grimwood S, Wafford K, Sandhu S, Whiting P, and McIlhinney RA (2001) Identification of molecular determinants that are important in the assembly of *N*-methyl-D-aspartate receptors. *J Biol Chem* **276:**18795–18803.

Nicole O, Docagne F, Ali C, Margaill I, Carmeliet P, MacKenzie ET, Vivien D, and Buisson A (2001) The proteolytic activity of tissue-plasminogen activator enhances NMDA receptor-mediated signaling. *Nat Med* **7:**59–64.

Paoletti P, Ascher P, and Neyton J (1997) High-affinity zinc inhibition of NMDA NR1-NR2A receptors. *J Neurosci* **17:**5711–5725.

Paoletti P, Perin-Dureau F, Fayyazuddin A, Le Goff A, Callebaut I, and Neyton J (2000) Molecular organization of a zinc binding N-terminal modulatory domain in a NMDA receptor subunit. *Neuron* **28:**911–925.

Pasternack A, Coleman SK, Jouppila A, Mottershead DG, Lindfors M, Pasternack M, and Keinanen K (2002) α-Amino-3-hydroxy-5-methyl-4-isoxazolepropionic acid (AMPA) receptor channels lacking the N-terminal domain. *J Biol Chem* **277:**49662–49667.

Perin-Dureau F, Rachline J, Neyton J, and Paoletti P (2002) Mapping the binding site of the neuroprotectant Ifenprodil on NMDA receptors. *J Neurosci* **22:**5955–5965.

Priestley T, Laughton P, Myers J, Le Bourdelles B, Kerby J, and Whiting PJ (1995) Pharmacological properties of recombinant human *N*-methyl-D-aspartate receptors comprising NR1a/NR2A and NR1A/NR2B subunit assemblies expressed in permanent transfected mouse fibroblast cells. *Mol Pharmacol* **48:**841–848.

Rachline J, Perin-Dureau F, Le Goff A, Neyton J, and Paoletti P (2005) The micromolar zinc-binding domain on the NMDA receptor subunit NR2B. *J Neurosci* **25:**308–317.

Sadtler S, Laube B, Lashub A, Nicke A, Betz H, and Schmalzing G (2003) A basic cluster determines topology of the cytoplasmic M3–M4 loop of the glycine receptor α1 subunit. *J Biol Chem* **278:**16782–16790.

Traynelis SF, Burgess MF, Zheng F, Lyuboslavsky P, and Powers JL (1998) Control of voltage-independent zinc inhibition of NMDA receptors by the NR1 subunit. *J Neurosci* **18:**6163–6175.

Tsirka SE, Gualandris A, Amaral DG, and Strickland S (1995) Excitotoxin-induced neuronal degeneration and seizure are mediated by tissue plasminogen activator. *Nature* **377:**340–344.

Williams K (1996) Separating dual effects of zinc at recombinant *N*-methyl-D-aspartate receptors. *Neurosci Lett* **215:**9–12.

Yao Y and Mayer ML (2006) Characterization of a soluble ligand binding domain of the NMDA receptor regulatory subunit NR3A. *J Neurosci* **26:**4559–4566.

Zheng F, Erreger K, Low CM, Banke T, Lee CJ, Conn PJ, and Traynelis SF (2001) Allosteric interaction between the amino terminal domain and the ligand binding domain of NR2A. *Nat Neurosci* **4:**894–901.

Address correspondence to: Bodo Laube, Technische Universität Darmstadt, AG Molekulare und zelluläre Neurophysiologie, Schnittspahnstr. 3, 64287 Darmstadt, Germany. E-mail: laube@mpih-frankfurt.mpg.de